

Highly Selective Suppression of Melanoma Cells by Inducible DNA Cross-Linking Agents: Bis(catechol) Derivatives

Minghui Bai,[†] Jing Huang,[†] Xiaolong Zheng,[†] Zhibin Song,[†] Miru Tang,[†]
Wuxiang Mao,[†] Libo Yuan,[†] Jun Wu,[†] Xiaocheng Weng,[†] and Xiang Zhou^{*†‡}

College of Chemistry and Molecular Sciences, State Key Laboratory of Virology, Wuhan University, Hubei, Wuhan 430072, P. R. China, and State Key Laboratory of Natural and Biomimetic Drugs, Peking University, Beijing 100083, P. R. China

Received July 26, 2010; E-mail: xzhou@whu.edu.cn

Abstract: A series of bis(catechol) quaternary ammonium derivatives were designed and synthesized. We investigated their ability to cross-link DNA induced by tyrosinase and found that the *o*-quinone is key intermediate in the process by using the nucleophile 3-methyl-2-benzothiazolinone hydrazone (MBTH) in the tyrosinase assay. Their cytotoxicities to B16F1, Hela, and CHO cells were tested by MTT assays. The specific and potent abilities to kill the tyrosinase-efficient melanoma cells kindled our interest in exploring the relationship between their abilities of cross-linking DNA and their selective cytotoxicities to cells. Through an integrated approach including intracellular imaging for detection of the dihydroxyphenyl groups, alkaline comet assays, and γ -H2AX immunofluorescence assays, the speculation was confirmed. The bis(catechol) quaternary ammonium derivatives showed notable cell selectivity because they displayed cytotoxicities after being oxidized by tyrosinase, and they were able to target the DNA efficiently in the tyrosinase-efficient melanoma cells, forming both alkylated and cross-linked species.

Introduction

Traditional chemotherapy and radiation are effective therapies; however, the lack of selective cytotoxicity often results in intolerable side effects. Thus, there is an urgent need for improved treatment.¹ Melanoma is a malignant tumor that originates in melanocytes, and these cells produce the pigment melanin.² Tyrosinase, an enzyme that is highly expressed in malignant tumors, mediates the biosynthesis of melanin. Many tyrosinase inhibitors from artificial or natural sources selectively block melanogenic pathways.³ Natural tyrosinase inhibitors such as flavonoids⁴ are generally free of harmful side effects and induce significant inhibition of tyrosinase activity. Many groups have reported the selective treatment of malignant melanoma using melanocyte-directed enzyme prodrug therapy (MDEPT).⁵ The prodrug has a catechol or phenolic moiety that permits tyrosinase oxidation before the release of the active agent.

Therefore, these strategies targeting tyrosinase could induce tyrosinase expression in melanocytes.

In our previous study,⁶ we reported that bis(catechol) quaternary ammonium derivatives may be used as potent, water-soluble, and tyrosinase-dependent DNA cross-linking agents (Scheme 1). DNA cross-linking is a common chemical process that is a useful chemical tool. DNA cross-linking agents covalently bind the complementary strands of the DNA double helix, preventing DNA replication and inducing cytotoxic DNA double-strand breaks (DSBs).⁷ Endogenous enzyme-inducible cross-linking agents have promising therapeutic potential because of their moderate inducing conditions and low side effects.⁸ If a selective therapeutic strategy is developed, the bis(catechol) quaternary ammonium derivatives may specifically target malignant cells. These agents may be highly toxic to tumor cells as a result of the formation of intra- and/or interstrand adducts. Our approach is similar to two previous strategies that depend on the activation of tyrosinase, which is highly expressed in melanoma cells. In this paper, we present a series of bis(catechol) quaternary ammonium derivatives that effectively target the nuclei of melanoma cells. These derivatives have two catechol units that are linked through various aliphatic and aromatic chains and have the capacity to cross-link DNA.

[†] Wuhan University.

[‡] Peking University.

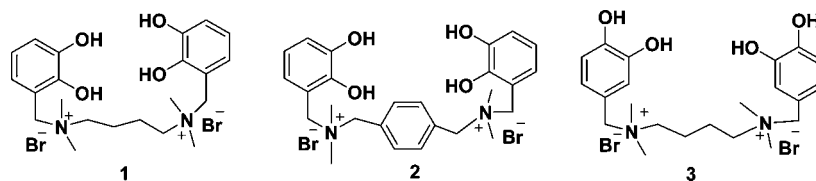
- (1) Kyrgidis, A.; Tzellos, T.; Triaridis, S. *J. Carcinog.* **2010**, *9*, 3–18.
- (2) Ye, Y.; Chou, G. X.; Mu, D. D.; Wang, H.; Chu, J. H.; Leung, A. K. M.; Fong, W. F.; Yu, Z. L. *J. Ethnopharmacol.* **2010**, *129*, 387–390.
- (3) (a) Yamaoka, Y.; Ohguchi, K.; Itoh, T.; Nozawa, Y.; Akao, Y. *Biosci., Biotechnol., Biochem.* **2009**, *73*, 1429–1431. (b) Ghani, U.; Ullah, N. *Bioorg. Med. Chem.* **2010**, *18*, 4042–4048.
- (4) (a) Seo, Y. K.; Jung, S. H.; Song, K. Y.; Park, J. K.; Park, C. S. *Eur. Food. Res. Technol.* **2010**, *231*, 163–169. (b) Lu, Y. H.; Chen, J.; Wei, D. Z.; Wang, Z. T.; Tao, X. Y. *J. Enzyme Inhib. Med. Chem.* **2009**, *24*, 1154–1160.
- (5) (a) Perry, M. J.; Mendes, E.; Simplício, A. L.; Coelho, A.; Soares, R. V.; Iley, J.; Moreira, R.; Francisco, A. P. *Eur. J. Med. Chem.* **2009**, *44*, 3228–3234. (b) Jordan, A. M.; Khan, T. H.; Malkin, H.; Osborn, H. M. I.; Photiou, A.; Riley, P. A. *Bioorg. Med. Chem.* **2001**, *9*, 1549–1558.

(6) Song, Z. B.; Weng, X. C.; Weng, L. W.; Huang, J.; Wang, X. L.; Bai, M. H.; Zhou, Y. Y.; Yang, G. F.; Zhou, X. *Chem.—Eur. J.* **2008**, *14*, 5751–5754.

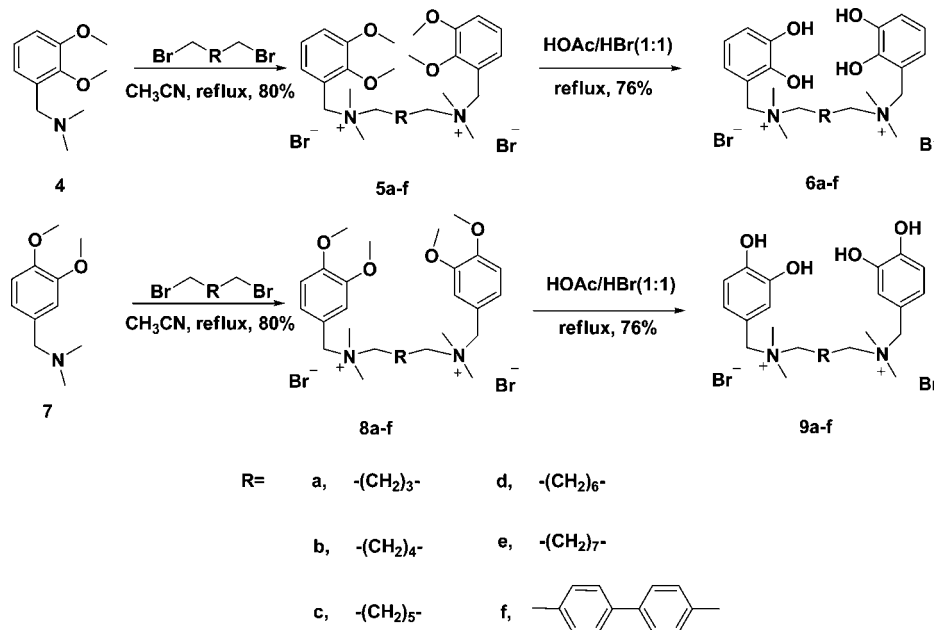
(7) (a) Wang, P.; Song, Y.; Zhang, L. X.; He, H. P.; Zhou, X. *Curr. Med. Chem.* **2005**, *12*, 2893–2913. (b) Noll, D. M.; Mason, T. M.; Miller, P. S. *Chem. Rev.* **2006**, *106*, 277–301. (c) Skladanowski, A.; Koba, M.; Konopa, J. *Biochem. Pharmacol.* **2001**, *61*, 67–72.

(8) Celli, C. M.; Jaiswal, A. K. *Cancer Res.* **2003**, *63*, 6016–6025.

Scheme 1. Structures of Bis(catechol) Derivatives



Scheme 2. Synthesis of Bis(catechol) Derivatives



A series of cellular assays were also used to investigate the relationship between DNA cross-linking activity and selective cytotoxicity.

Results and Discussion

Synthesis of Bis(catechol) Quaternary Ammonium Derivatives. The symmetrical bis(catechol) quaternary ammonium derivatives **6a–f** and **9a–f** were prepared as shown in Scheme 2. All of the new compounds were fully characterized by high-resolution mass spectrometry (HRMS) and ¹H and ¹³C NMR spectroscopy.

DNA Cross-Linking. The DNA–DNA cross-linking abilities of the 12 bis(catechol) quaternary ammonium derivatives were investigated using a negatively supercoiled plasmid DNA (pBR322) by denatured alkaline agarose gel electrophoresis. The nonreacted plasmid was present in its single-stranded DNA (ssDNA) form. The interstrand cross-linking (ISC) activities of the compounds were evident as a DNA cross-linking bands, which run slightly slower than the ssDNA form. As shown in Figure 1A, ISC was more efficacious for the 3,4-dihydroxy derivatives **9a–f** than for the 2,3-dihydroxy derivatives **6a–f**. This is consistent with our previously published results that 3,4-dihydroxy substitutions in the benzene ring may be preferable for tyrosinase-induced DNA cross-linking.⁶ Compound **9f** produced nearly 100% DNA cross-linking at a concentration of 15 μM after incubation for 30 min with tyrosinase. Relative to our earlier published results,⁶ compound **2** (Scheme 1) produced only 30% DNA cross-linking at a concentration of 20 μM. The biphenyl-linker-containing compound **9f** had the most potent ISC properties. It was about 4-fold more efficient than compound **2** as a DNA cross-linking agent.

The cross-linking percentages measured for different compounds are shown in Figure 1B, where they are expressed as mean values of three individual experiments conducted in triplicate. The results show that the 3,4-dihydroxy derivatives **9a–f** have higher DNA cross-linking abilities than the 2,3-dihydroxy derivatives **6a–f**. On the other hand, the compounds with biphenyl linkers have higher DNA cross-linking abilities than those with aliphatic linkers. This probably results from the fact that the biphenyl core preferably binds and reacts with the DNA helix. In these cases, the 3,4-dihydroxy derivative with biphenyl core, **9f**, is the most efficient cross-linking agent.

Proposed Mechanism of Tyrosinase Oxidation between DNA and Catechol. These DNA cross-linking agents can form an *o*-quinone intermediate induced by tyrosinase. In order to determine the formation of *o*-quinone methide, we performed the 3-methyl-2-benzothiazolinone hydrazone (MBTH) color test to measure the formation of the intermediate *o*-quinone in our current study.⁹ The dihydroxyphenyl groups were oxidized by tyrosinase into *o*-quinones, which reacted with MBTH by a Michael reaction to form a dark-pink pigment (shown in Figure 2). The formation of the quinone intermediate was monitored by UV–vis spectroscopy. The addition of MBTH to the reaction resulted in the formation of MBTH–*o*-quinone adducts, which are intensely colored (Figure 2A). As shown in Figure 2B, the maximum absorption of compound **9f** and MBTH is at 260 nm. After reaction with tyrosinase for 1 h, a peak at 360 nm appeared, indicating the structural change of the dihydroxyphenyl

(9) (a) McMahon, A. M.; Doyle, E. M.; O'Connor, K. E. *Enzyme Microb. Technol.* **2005**, *36*, 808–812. (b) Winder, A. J.; Harris, H. *Eur. J. Biochem.* **1991**, *198*, 317–326.

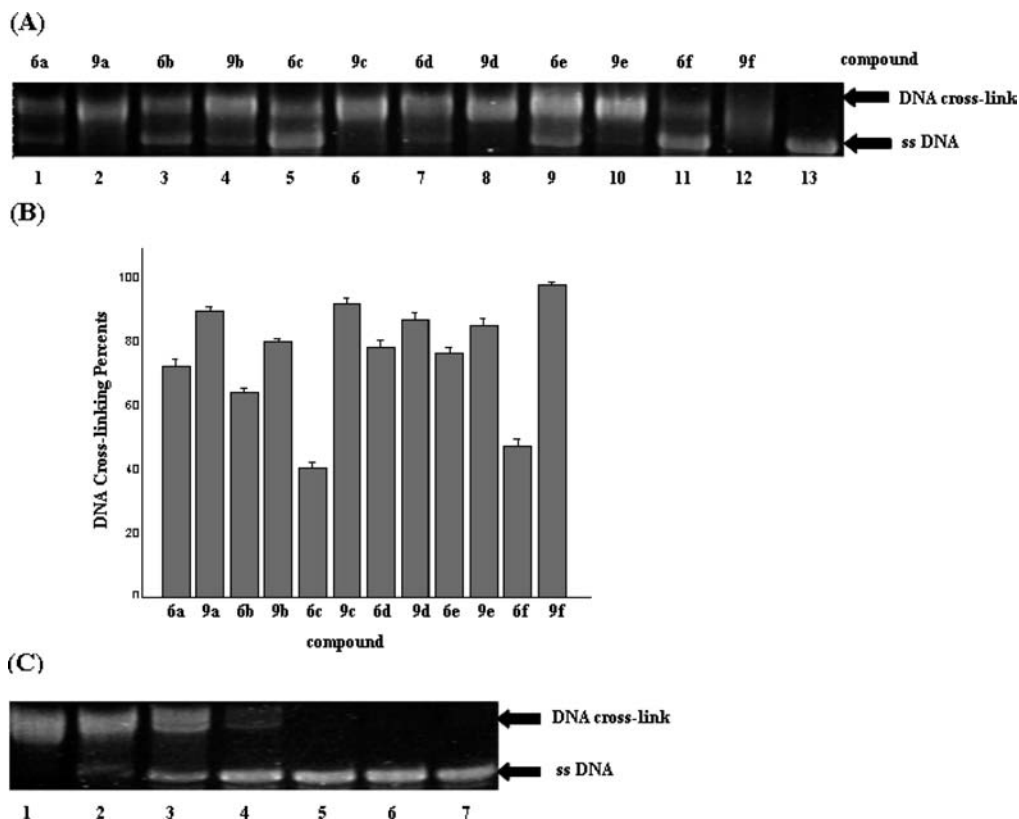


Figure 1. Agarose gel electrophoresis of 12 bis(catechol) quaternary ammonium salt derivatives (tyrosinase oxidation). (A) The concentrations of drug and tyrosinase were fixed at 20 μ M and 40 units, respectively. Lanes 1–12: 0.7 μ g of pBR322 + 20 μ M 6a–6f, 9a–9f + tyrosinase. Lane 13: 0.7 μ g of pBR322 + tyrosinase. (B) Histogram of cross-linking percentages for different compounds. The standard deviations of the cross-linking percentages were obtained from three individual experiments. (C) Concentration dependence of compounds 9f. Lanes 1–4: concentrations of 9f are 15, 10, 5, 1 μ M. Lane 5: 0.7 μ g of pBR322 + 15 μ M 9f. Lane 6: 0.7 μ g of pBR322 + tyrosinase. Lane 7: 0.7 μ g of pBR322.

nyl groups in compound 9f to *o*-quinones (Figure S1 in the Supporting Information).

The mechanism of catechol oxidation by tyrosinase has been clearly researched.¹⁰ The key point is that catalysis of the reaction by tyrosinase depends on the ability of the substrate to bind to the tyrosinase active site. If the substrate can bind well with the tyrosinase active site, tyrosinase will oxidize the substrate efficiently. For our results, 9a–f have structures very similar to that of 3,4-dihydroxyphenylalanine (DOPA), which is the natural oxidation substrate of tyrosinase.¹¹ Therefore, this suggested that 9a–f should have a similar ability as DOPA to bind to the active site of tyrosinase and thus that tyrosinase should oxidize substrates 9a–f efficiently. In contrast, compounds 6a–f could not be oxidized efficiently by tyrosinase because of their weak binding abilities to tyrosinase. On the basis of the tyrosinase-specific catalytic mechanism, tyrosinase catalyzes the conversion of the bis(catechol) to the corresponding bis(quinone) in two steps. First, two protons are abstracted from each of the catechol groups, and the deprotonated catechol oxygen atoms bind to two Cu(II) ions of tyrosinase in the active

site.¹⁰ The resulting intermediate has the advantage of easy translation of electrons, resulting in the formation of the deoxy form of tyrosinase and the bis(quinone). The bis(quinone) then has the corresponding position for the nucleophilic reaction by DNA, which finally results in DNA cross-links (Figure 3).

Evaluation of the Cytotoxicities of the Bis(catechol) Quaternary Ammonium Derivatives in Three Cell Lines. To characterize the activity of these cross-linking agents in biological systems, we determined their toxicities in the B16F1 murine melanoma cell line (which highly expresses tyrosinase) and in Chinese hamster ovary (CHO) and Hela cells (tyrosinase-deficient cell lines).¹² The cell damage was assessed using MTT assays, and the results for each compound are shown in Table 1. Each compound induced a high level of toxicity in B16F1 cells but exhibited relatively low toxicities in the tyrosinase-deficient CHO and Hela cell lines. Compound 9f potently induced cytotoxicity in B16F1 cells with an IC_{50} of ~ 7 μ M. These experiments demonstrate that the bis(catechol) quaternary ammonium derivatives selectively target high-tyrosinase-expressing B16F1 cells. This mechanism is probably due to DNA alkylation or cross-linking, which requires tyrosinase as an oxidative agent.

Intracellular Imaging for Detection of the Dihydroxyphenyl Groups. Boron dipyrromethene (BODIPY) dyes are commonly used as visible fluorescence probes in intracellular imaging applications.¹³ To test whether the dihydroxyphenyl groups were oxidized by tyrosinase in B16F1 cells, we used BODIPY-modified catechol 13 (whose synthesis is shown in Scheme S1

(10) (a) Muñoz-Muñoz, J. L.; García-Molina, F.; García-Ruiz, P. A.; Molina-Alarcón, M.; Tudela, J.; García-Cánovas, F.; Rodríguez-López, J. N. *Biochem. J.* **2008**, *416*, 431–440. (b) Cooksey, C. J.; Garratt, P. J.; Land, E. J.; Ramsden, C. A.; Riley, P. A. *Biochem. J.* **1998**, *333*, 685–691.

(11) (a) Decker, H.; Schweikardt, T.; Tuzek, F. *Angew. Chem., Int. Ed.* **2006**, *45*, 4546–4550. (b) Garaud, M.; Pei, D. *J. Am. Chem. Soc.* **2007**, *129*, 5366–5367. (c) Mirica, L. M.; Vance, M.; Rudd, D. J.; Hedman, B.; Hodgson, K. O.; Solomon, E. I.; Stack, T. D. *Science* **2005**, *308*, 1890–1892. (d) Solomon, E. I.; Sundaram, U. M.; Machonkin, T. E. *Chem. Rev.* **1996**, *96*, 2563–2605.

(12) Jordan, A. M.; Khan, T. H.; Osborn, H. M. I.; Photiou, A.; Riley, P. A. *Bioorg. Med. Chem.* **1999**, *7*, 1775–1780.

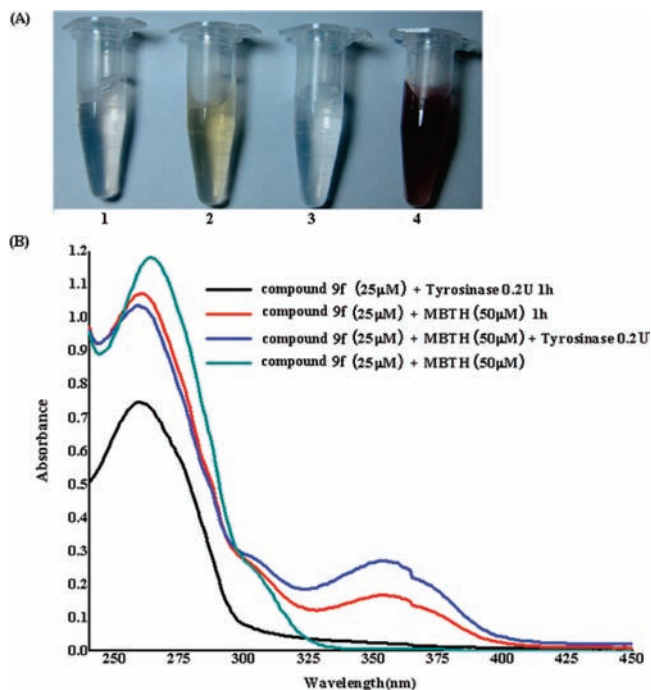


Figure 2. (A) MBTH color test based on trapping of the intermediate *o*-quinones formed from compound **9f**. The concentrations of **9f**, MBTH, and tyrosinase were fixed at 500 μM , 1 mM, and 40 units, respectively. (1) **9f** + MBTH; (2) **9f** + tyrosinase; (3) MBTH + tyrosinase; (4) **9f** + MBTH + tyrosinase. (B) Absorption spectra of **9f** (25 μM) and MBTH (50 μM) before and after reaction with tyrosinase (0.2 units/mL) for 1 h at 37 $^{\circ}\text{C}$. The spectra were measured using a phosphate buffer solution (pH 6.4) as a blank.

in the Supporting Information) as a fluorescent dye to monitor the spatiotemporal distribution of the dihydroxyphenyl groups and cellular processes of DNA cross-linking.

The fluorescence of **13** was weak. After oxidation by tyrosinase in a phosphate buffer solution, the fluorescence of **13** increased ~ 2 -fold (Figure S2 in the Supporting Information). B16F1 cells loaded with **13** elicited bright-green fluorescence in cytoplasm, whereas HeLa and CHO cells gave weak fluorescence responses (Figure 4). This implies that the dihydroxyphenyl group can be activated by the tyrosinase in B16F1 cells. The catechol dye **13** had little effect on HeLa and CHO cells because of the nonoxidizing environment.

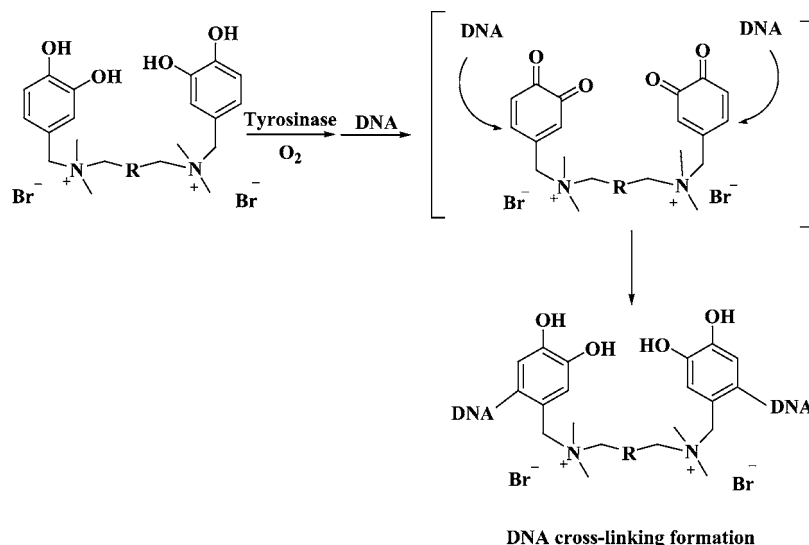


Figure 3. Proposed mechanism of tyrosinase oxidation between DNA and catechol.

Table 1. Cytotoxicities (IC_{50} Values in μM) of the Bis(catechol) Quaternary Ammonium Salt Derivatives in the Three Cell Lines

compound	IC_{50} (μM)		
	B16 F1	HeLa	CHO
6a	15.09 ± 1.49	>50	>50
9a	13.65 ± 1.13	>50	>50
6b	20.98 ± 1.76	>50	>50
9b	18.68 ± 0.98	>50	>50
6c	27.98 ± 2.04	>50	>50
9c	21.12 ± 1.33	>50	>50
6d	18.09 ± 1.52	>50	>50
9d	17.98 ± 1.28	>50	>50
6e	10.07 ± 1.12	>50	>50
9e	9.67 ± 1.08	>50	>50
6f	7.88 ± 1.65	>50	>50
9f	7.29 ± 0.75	>50	>50

We also found that the fluorescence of BODIPY-modified catechol **13** in the nucleus of the B16F1 cell was very weak. The fluorescence quenching of **13** in the nucleus of the B16F1 cell may have resulted from DNA alkylation or cross-linking with **13** after it was oxidized by the tyrosinase. To confirm our hypothesis, the fluorescence of **13** in a genomic DNA extraction mixture was tested *in vitro*. We found that with increasing concentration of genomic DNA extract from B16F1 cells, the fluorescence intensity of **13** at the characteristic peak near 508 nm dramatically decreased (Figure S3 in the Supporting Information). This may explain that the faintness of the fluorescence of **13** in the nucleus of the B16F1 cell is the result of the interaction between the cross-link agent and nuclear DNA.

Since the oxidation of the dihydroxyphenyl groups occurs in the cytoplasm, the oxidation product *o*-quinone might react with other nucleophiles in cells (e.g., reduced glutathione,¹⁴ a thiol-containing tripeptide) rather than nucleus DNA. Glutathione is well-known for its redox capabilities and is widely distributed in cells.¹⁵ *In vitro*, we found that the fluorescence of BODIPY-modified catechol **13** increased after addition of the tyrosinase/reduced glutathione mixture (Figure S4 in the Supporting Information). Thus, the faintness of the fluorescence in the nucleus was not due to quenching of the *o*-quinone by glutathione but instead resulted from DNA alkylation or cross-linking in the nucleus.

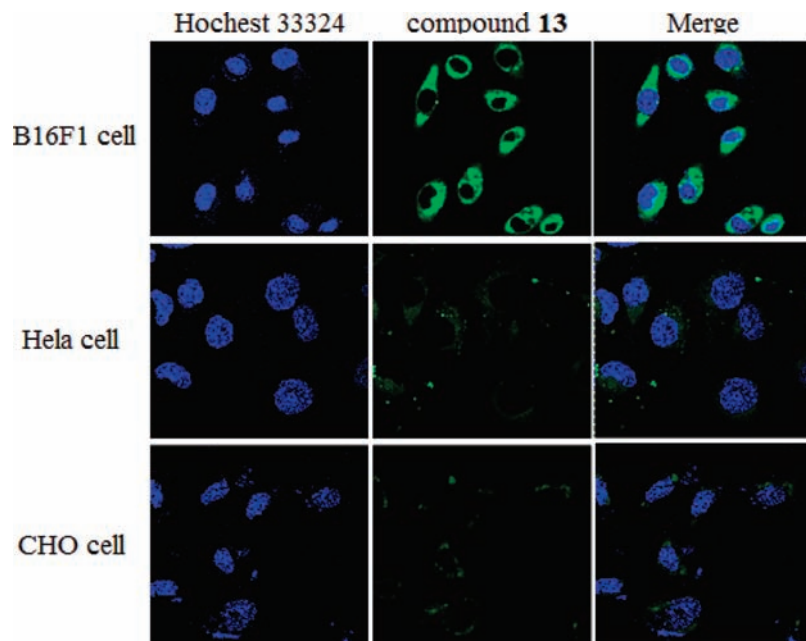


Figure 4. Confocal microphotographs of three different cells after treatment with compound **13** (500 nM) followed by staining with Hoechst-33324 (blue).

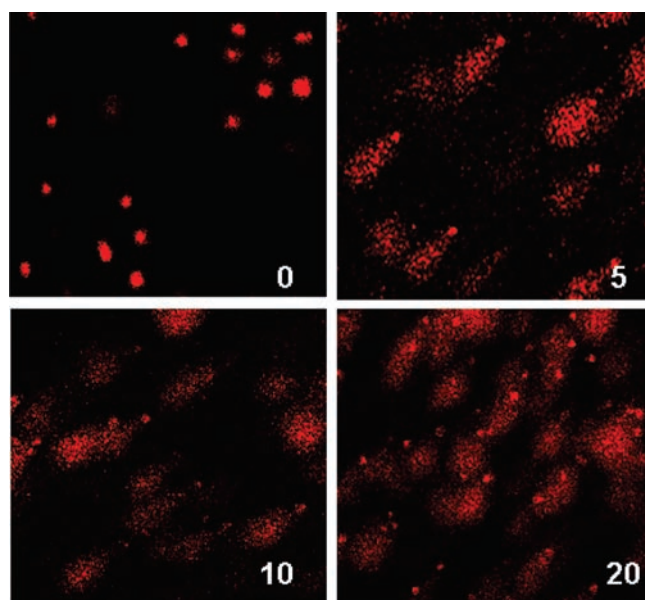


Figure 5. Alkaline comet assay for B16F1 cells treated with compound **9f**. Cells were incubated with increasing concentrations of compound **9f** (0, 5, 10, and 20 μ M) for 48 h.

Bis(catechol) Quaternary Ammonium Derivative **9f Produces DNA Alkylation in Cell Systems.** DNA interstrand cross-links are absolute blocks to replication and transcription and may also give rise to DSBs during its repair. DNA DSBs are considered to be the most dangerous form of DNA damage.¹⁶ We performed an alkaline comet assay¹⁷ to confirm the DNA damage induced by bis(catechol) quaternary ammonium derivative **9f** in the cellular environment (Figure 5).

In the control untreated cells, DNA damage was not detected, and the high-molecular-weight supercoiled DNA remained intact. As the drug concentration was increased, a fixed number of random DNA strand breaks produced short DNA fragments that were observed as comet images. At a dose of 20 μ M,

bis(catechol) **9f** resulted in a shorter comet tail. This result indicates that (1) **9f** reached its target DNA inside the cells; (2) at low doses, **9f** alkylated chromosomal DNA; and (3) at higher concentrations, **9f** displayed efficient cross-linking ability, which was observed as a tail with a wide range of lengths. However, less damage and less DNA migration were observed in the HeLa and CHO cells treated with high concentrations of compound **9f** (Figure S5 in the Supporting Information).

Immunofluorescence Microscope Detection of γ -H2AX Foci. γ -H2AX immunofluorescence microscopy is a reliable and sensitive method for measuring DNA damage. The histone H2AX is rapidly phosphorylated following exposure of cells to DSB-inducing agents.¹⁸ Within minutes of DSB generation, γ -H2AX molecules are phosphorylated in large chromatin domains that flank the DNA DSBs; these domains can be observed by immunofluorescence microscopy and are termed γ -H2AX foci.¹⁹

It has been reported that the formation of DNA interstrand cross-links can be converted to DSBs when a DNA replication fork is encountered or during its repair.¹⁶ As shown in Figure 6A, treatment with compound **9f** triggered DNA damage in the nucleus. The DNA damage induced by **9f** was evidenced by the presence of γ -H2AX foci, which were absent in the control cells. In contrast, treatment of HeLa and CHO cells with 20 μ M **9f** for 48 h did not induce noticeable DNA damage (Figure S6 in the Supporting Information). Furthermore, treatment with compound **9f** caused nucleus budding in B16F1 cells (Figure S7 in the Supporting Information). Nuclear condensation and fragmentation, the typical characteristics of apoptosis, were observed only in B16F1 cells. These results indicate that the tyrosinase-activated cross-linking induces cytotoxic DNA damage and give further evidence that these catechol derivatives may specifically interact with the B16F1 cells as a result of DNA alkylation only in the B16F1 cells.

Conclusion

In summary, we have successfully synthesized a series of bis(catechol) quaternary ammonium derivatives that efficiently

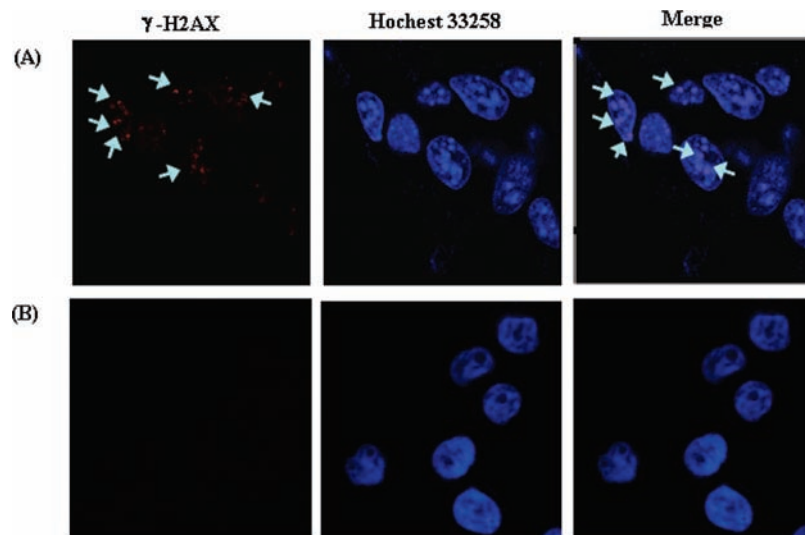


Figure 6. γ -H2AX immunofluorescence in B16F1 cells after incubation (A) with and (B) without treatment with 5 μ M **9f** for 48 h. The arrows indicate γ -H2AX foci (red) and the Hoechst-33258 dye (blue) localizes the nuclear DNA.

cross-link DNA through the formation of bis(*o*-quinone) by tyrosinase-dependent oxidation. We have shown that DNA cross-linking may lead to specific and potent targeting of tyrosinase-expressing cells. This novel therapeutic strategy induces cytotoxicity to melanoma cells. This may well provide a possible chemotherapy for melanoma that employs tyrosinase-activated agents that can induce cytotoxic DNA double-strand breaks.

Experimental Section

Materials and Apparatus. The following compounds and reagents were commercially available: tyrosinase mushroom (Sigma), MBTH (Sigma), reduced glutathione (Sigma), MEM (HyClone, Thermo Scientific), RPMI 1640 medium (GIBCO), fetal bovine serum (FBS, HyClone), penicillin and streptomycin (Invitrogen), MTT (Sigma), γ -H2AX (phosphor S139) rabbit polyclonal (ab1174, Abcam), Hoechst-33258 (Calbiochem), Hoechst-33324 (Calbio-

chem), and propidium iodide (Sigma-Aldrich). UV spectra were measured on a Shimadzu 2550 UV-vis double-beam spectrophotometer. Fluorescence spectra were collected on PerkinElmer LS 55 fluorimeter. The excitation and emission slit widths were both set to 10 nm. All of the cell imaging was performed with a Nikon confocal laser scanning microscope (TE2000, Japan). Images and merges were obtained with EZ-C1 software.

All other chemicals were purchased from Sigma-Aldrich and used as received. All new compounds were fully characterized by HRMS and ^1H NMR and ^{13}C NMR spectroscopy. ^1H and ^{13}C NMR spectra were recorded on Varian Mercury 300 and 600 spectrometers, respectively. Chemical shifts were reported as δ values relative to the internal standard tetramethylsilane. HRMS spectra were recorded on a Bruker APEX IV (7.0 T) ESI-QTPF mass spectrometer (Bruker Daltonik GmbH, Bremen, Germany) and an APEX II FT-ICR instrument.

General Procedure for the Synthesis of 2,3-Dihydroxy Derivatives 6a–f and 3,4-Dihydroxy Derivatives 9a–f. The symmetrical bis(catechol) quaternary ammonium derivatives **5a–f** and **8a–f** were prepared through condensation of the corresponding dibromo compounds with (2,3-dimethoxybenzyl)dimethylamine (**4**) and (3,4-dimethoxybenzyl)dimethylamine (**7**), respectively. Demethylation reactions of compounds **5a–f** and **8a–f** were performed in 1:1 HOAc/40% HBr cosolvents, affording the compounds **6a–f** and **9a–f** in good yields. Compounds **4** and **7** were synthesized according to our previously published procedure.⁶ 4,4'-Bis(bromomethyl)biphenyl was synthesized according to a previously published procedure.²⁰

Alkaline Agarose Gel Electrophoresis Assay. The duplex DNA was linearized by restriction endonuclease digestion with EcoR I. DNA cross-linking experiments were carried out in 10 mM phosphate buffer (pH 6.4). Samples were incubated with 40 units of mushroom tyrosinase in the presence of atmospheric O_2 at 37 $^\circ\text{C}$ for 30 min. The crude reaction mixtures were loaded onto a denaturing 0.9% alkaline agarose gel. The gel was stained in ethidium bromide (0.5 $\mu\text{g}/\text{mL}$) for 30 min and subsequently washed in water for 10 min. Gels were visualized by UV and photographed using a Vilber Lourmat video system.

BMTH Assay. Compound **9f** (500 μM) was incubated with 40 units of mushroom tyrosinase in the presence of atmospheric O_2 and 1 mM MBTH for 1 h. MBTH solutions were freshly prepared before use. The spectrum was measured on UV-vis spectrophotometer.

- (13) (a) Domaille, D. W.; Zeng, L.; Chang, C. J. *J. Am. Chem. Soc.* **2010**, *132*, 1194–1195. (b) Devaraj, N. K.; Hilderbrand, S.; Upadhyay, R.; Mazitschek, R.; Weissleder, R. *Angew. Chem., Int. Ed.* **2010**, *49*, 2869–2872.
- (14) (a) Pallardó, F. V.; Markovic, J.; García, J. L.; Viña, J. *Mol. Aspects Med.* **2009**, *30*, 77–85. (b) Gad, S. C. *Glutathione* **1998**, *2*, 53–54.
- (15) (a) Potters, G.; Jansen, M. A. K.; Horemans, N.; Guisez, Y.; Pasternak, T. *In Vitro Cell. Dev. Biol.: Plant* **2010**, *46*, 289–297. (b) Kudugunti, S. K.; Vad, N. M.; Whiteside, A. J.; Naik, B. U.; Yusuf, M. A.; Srivenugopal, K. S.; Moridani, M. Y. *Chem. Biol. Interact.* **2010**, *188*, 1–14. (c) Manini, P.; Napolitano, A.; Westerhof, W.; Riley, P. A.; d'Ischia, M. *Chem. Res. Toxicol.* **2009**, *22*, 1398–1405.
- (16) (a) Muniandy, P. A.; Liu, J.; Majumdar, A.; Liu, S.; Seidman, M. M. *Crit. Rev. Biochem. Mol. Biol.* **2010**, *45*, 23–49. (b) Sczepanski, J. T.; Jacobs, A. C.; Houten, B. V.; Greenberg, M. M. *Biochemistry* **2009**, *48*, 7565–7567. (c) Wood, R. D. *Environ. Mol. Mutagen.* **2010**, *51*, 510–526. (d) Hinz, J. M. *Environ. Mol. Mutagen.* **2010**, *51*, 582–603.
- (17) (a) Doria, F.; Richter, S. N.; Nadai, M.; Colloredo-Mels, S.; Mella, M.; Palumbo, M.; Freccero, M. *J. Med. Chem.* **2007**, *50*, 6570–6579. (b) Cederberg, H.; Henriksson, J.; Binderup, M. L. *Mutagenesis* **2010**, *25*, 133–138. (c) Eren, K.; Özmeriç, N.; Sardeş, S. *Clin. Oral Invest.* **2002**, *6*, 150–154.
- (18) (a) Kinner, A.; Wu, W. Q.; Staudt, C.; Iliakis, G. *Nucleic Acids Res.* **2008**, *36*, 5678–5694. (b) Cowell, I. G.; Sunter, N. J.; Singh, P. B.; Austin, C. A.; Durkacz, B. W.; Tilby, M. J. *PLoS One* **2007**, *10*, e1057.
- (19) (a) Gomez, D.; Wenner, T.; Brassart, B.; Douarre, C.; O'Donohue, M. F.; Khoury, V. E.; Shin-ya, K.; Morjani, H.; Trentesaux, C.; Riou, J. F. *J. Biol. Chem.* **2006**, *281*, 38721–38729. (b) Yao, K.; Wu, W.; Yu, Y. B.; Zeng, Q. L.; He, J. L.; Lu, D. Q.; Wang, K. J. *Invest. Ophthalmol. Visual Sci.* **2009**, *49*, 2009–2015.

- (20) Helms, A.; Heiler, D.; McLendon, G. *J. Am. Chem. Soc.* **1992**, *114*, 6227–6238.

Cell Culture. B16F1, HeLa, and CHO cell lines were purchased from China Center for Type Culture Collection (CCTCC). HeLa and CHO cell lines were grown in MEM medium, and B16F1 cells were grown in RPMI 1640 medium supplemented with 10% FBS and 1% penicillin and streptomycin.

Cell Survival Assay. Cells were harvested using trypsin and washed with PBS. The cells were added to the wells of a 96-well plate and incubated overnight for attachment at 37 °C in a 5% CO₂ incubator. The following day, cells were treated with the compounds (10 nM–50 mM) for 48 h. Control cells (without any compound) were treated under the exact same conditions. After the incubation period, cell survival was evaluated using an MTT assay: 10 μ L of a freshly prepared solution of MTT (5 mg/mL in PBS) was added to each well, and after 4 h of incubation, the medium was removed; after addition of 100 μ L of DMSO to each well, the optical density values were detected at 570 nm. Cytotoxicity data were expressed as IC₅₀ values. Data were expressed as mean values of three individual experiments conducted in triplicate.

Alkaline Comet Assay. Cells were plated (4×10^4 cells/well) onto six-well plates to a final volume of 2 mL and allowed an overnight period for attachment. Next, 1 μ L of each dilution of the tested compounds (0–20 μ M) was added per well, and the mixtures were incubated at 37 °C for 48 h. After 48 h of incubation, the medium was removed and replaced with HBSS solution, after which the cells were scraped off. A total of 10 μ L of cells was suspended in 65 μ L of 0.5% low-melting-point agarose and precoated with 0.5% normal-melting-point agarose. Cells were lysed overnight at 4 °C in cold lysis buffer (1% fresh Triton X-100, 2.5 M NaCl, 100 mM EDTA, and 10 mM Tris-HCl, pH 10.0). The agarose gels were then washed in water, incubated in alkaline electrophoresis buffer (300 mM NaOH and 1 mM EDTA at pH >13) for 30 min, and then subjected to electrophoresis in the same buffer at 25 V and 300 mA for 40 min. The gels were then rinsed with neutralization buffer (0.4 M Tris, pH 7.5) and left to air-dry, after which they were stained with 10 μ g/mL propidium iodide and incubated for 20 min. Finally, images were analyzed using a Nikon confocal laser scanning microscope.

γ -H2AX Immunofluorescence Assay. In the γ -H2AX immunofluorescence assay, cells plated on a 35 mm \times 10 mm glass-bottom cell culture dish were fixed and then washed in 0.5% Triton

X-100/PBS. The cells were then treated with permeabilization buffer [20 mmol/L Tris-HCl (pH 8), 0.5% Triton X-100, 50 mmol/L NaCl, 3 mmol/L MgCl₂, and 300 mmol/L sucrose] for 15 min at 37 °C, washed twice with PBS, and then antibody-stained with 1 μ g/mL γ -H2AX (phosphor S139) rabbit polyclonal at 4 °C overnight. The nuclear DNA was stained with 5 μ g/L Hoechst-33258. Secondary antibodies raised against rabbit were labeled with tetramethylrhodamine isothiocyanate, after which images were analyzed using a Nikon confocal laser scanning microscope.

Intracellular Dihydroxyphenyl Imaging. Cells were plated on a 35 mm \times mm glass-bottom cell culture dish and then treated with BODIPY-modified catechol **13** for 12 h. After the incubation period, the **13**-treated cells were rinsed with phosphate buffer, and 5 μ g/L Hoechst-33324 was added to stain the cell nuclei for 30 min at room temperature. Images were then analyzed using a Nikon confocal laser scanning microscope.

Acknowledgment. This work was supported by the National Science of Foundation of China (90813031, 30973605, 21072155, 20802055); the National Key Foundation for Infectious Diseases (Protection and treatment of AIDs, virus hepatitis, 2008ZX10003–005); the Fundamental Research Funds for the Central Universities; the State Key Laboratory of Applied Organic Chemistry, Lanzhou University; and the State Key Laboratory of Bioorganic and Natural Products Chemistry, Shanghai Institute of Organic Chemistry, the Chinese Academy of Sciences. We thank the editor and reviewers for their critical comments. We also thank Mr. Yangyang Zhou for his assistance in drawing the TOC graphic.

Supporting Information Available: Full synthesis procedures, characterization data for individual compounds, UV–vis and fluorescence spectra data, alkaline comet assay for HeLa and CHO cells, γ -H2AX immunofluorescence in CHO and HeLa cells, microphotographs of three different cells after treatment with the compounds, and proposed mechanism of the oxidative addition reaction between DNA and catechol. This material is available free of charge via the Internet at <http://pubs.acs.org>.

JA106637E